16

Opto-Electronic Study of SiC Polytypes: Simulation with Semi-Empirical Tight-Binding Approach

Amel Laref[1] and Slimane Laref[2]
[1]*Department of Physics and Astronomy, King Saud University, Riyadh 11451, Saudi Arabia and Department of physics, National Taiwan University, Taipei 106*
[2]*Université de Lyon, CNRS, Ecole Normale Supérieure de Lyon, Institut de Chimie de Lyon, Laboratoire de Chimie, Lyon*
[1]*Taiwan*
[2]*France*

1. Introduction

The recent growing scientific and technological interest on silicon carbide (SiC) arises from its peculiar physical properties, i.e., its mechanical, and chemical stability. Moreover, SiC is considered to be a promising material for electronic and optical devices. Microelectronic devices made of SiC can be used in high-power, high-speed, high temperature, high-frequency, and even hard-radiation application (1)-(4). The strong bonding between Si and C atoms in SiC makes this material very resistant to high temperature and radiation damage. In view of this extraordinary application potential a thorough knowledge of the structural and electronic properties of SiC is a matter of both ionic interest and technological importance. In addition to its traditional use as an abrasive (carborundum) there is currently much interest in materials made from SiC fibres, which compare well with their carbon fibre counterparts. Over a two hundred chemically stable semiconducting polytypes of SiC exist, they have a high bulk modulus and generally wide band gap. From such difference in stacking order it is possible to get almost 200 different crystal structures (1)-(10) of which the two extremes are the pure cubic polytype (with zinc blende structure) and the pure hexagonal one (with wurtzite structure). SiC is the most prominent of a family of close packed materials which exhibit a one dimensional polymorphism called polytypism. In addition, numerous hexagonal and rhombohedral structures (11)-(19) of SiC have been identified in addition to the common cubic form. In fact, SiC is one of the few compounds which form many stable and long-range ordered modifications, so-called polytypes (11)-(17). Previously, SiC has been subject to many theoretical studies. With this respect, a variety of structural, electronic and optical properties in SiC have been investigated by many theoretical groups (12)-(15) and the results can be related to the experimental works (7)-(10). In the last years, first-principle calculations have been applied to determine the ground-state properties of cubic and hexagonal polytypes of SiC (19)-(53). Based on previous theoretical works, the high-pressure behavior (18)-(33), and the effect of atomic relaxation on structural properties

were also investigated (14)-(18). Some attempts towards the explanation of the existence of a large number of metastable SiC polytypes have been also undertaken (14)-(37). The electronic band structures of some SiC polytypes have been calculated by several groups (14)-(47). Further studies went deep into the optical properties of SiC polytypes (14)-(33). The optical and spectroscopic properties of SiC polymorphs have also been investigated by many groups both experimentally (7)-(14) and theoretically (19)-(25). Due to the problem of sample availability, most measurements were on 6H-SiC and 3C-SiC (54)-(57). Very recently, some measurements on 4H-SiC have also been reported (58)-(61). There are considerable variations in the measured optical properties mainly because the photon energy is limited to less than 6.6 eV using the popular ellipsometry technique. The use of vacuum-ultraviolet (VUV) spectroscopy can extend the energy range significantly and so far has only been carried out on 6H-SiC (57). Recent advances in crystal growth of SiC have allowed the study of the optical properties of different polytypes (54)-(60). In addition, tight-binding (TB) method has proven to be very useful for the study of both semiconductors and metallic systems, especially in systems which are too large to be studying via ab-initio techniques. This method is about 2 or 3 orders of magnitude faster than the ab initio formulations, and at the same time it describes with suitable accuracy the electronic structure of the systems. The computational efficiency of the TB method derives from the fact that the Hamiltonian can be parametrized. Furthermore, the electronic structure information can be easily extracted from the TB hamiltonian, which, in addition, also contains the effects of angular forces in a natural way. In order to use a more realistic method, we present a TB model with sp^3s^* basis, representing exact curvatures of lowest conduction bands. The TB approach is standard and widely used for the electronic properties of a wide variety of materials. In the present contribution we overview our most recent results on the electronic structures and optical properties of SiC polytypes (62). Hence, the SiC polytypes can be considered as natural superlattices, in which the successive layers consist of Hexagonal SiC material of possibly different width. Our TB model can treat SiC polytypes as superlattices consisting hexagonal bulk-like blocks. We have investigated to which extent it is acceptable approximation for existing polytypes when various of nH-SiC crystal are used to present polytype superlattices. Indeed, this is an accurate approximation by building blocks consist of n-layers of nH-SiC. By representing in general the polytypes as superlattices, we have applied our recent TB model (62) that can treat the dimensions of the superlattice. Within this model we take for each sublayer linear combination of atomic orbitals of hexagonal SiC which are subsequently matched at the interfaces to similar combinations in the adjacent sublayers by using the boundary conditions. Polytypic superlattices, in comparison with heterostructure superlattices, have two important additional features, namely (i) the polytypes are perfectly lattice-matched superlattices and (ii) the polytypes have an energy band offset between adjacent layers equal to zero by definition. We can obtain with our TB model the band structures and particularly the energy band gaps of SiC polytypes and their wave functions. Our recent TB model (62) is very efficient when extended it to investigate the electronic properties of wurtzite (wz) superlattices in (0001) direction.

This chapter is organized as follows: Section 1 provides a review for the large band-gap SiC based semiconductor device technology. In the next section we present the different polytism of SiC. A fundamental concept of the TB theory for SiC polytypes is described in section 3. Our recent TB model is specifically applied to study the electronic and optical properties of SiC polytypes and it can be applied to nH-SiC wurtzite superlattices. The present approach is also suited for all wurtzite semiconductor superlattices and large complex unit cells which

can be treated where the transferability of the hopping parameters is required. Section 4 deals with some of our recent results of the electronic and optical properties of SiC polytypes. To reach these, we analyzed this statement in terms of optoelectronic properties of SiC polytypes. Finally in section 5 we summarize and conclude.

2. A review of the large band-gap SiC based semiconductor device technology

The recent surge of activity in wide band-gap semiconductors has arisen from the need for electronic devices capable of operation at high power levels, and high-radiation resistance, and separately, a need for optical materials, especially emitters, which are active in the blue and ultraviolet (UV) wavelengths (63)-(69). In this aspect, there has been renewed interest in SiC as one of the wide band gap compounds with great potential for the next generation of electronic devices operating at high temperature (61)-(68). This compound has been also used primarily in light-emitting diodes. SiC's intrinsic material properties as well as its existence in various polytypes have led to a revival of technological interest. Crystal growth of SiC polytypes has recently shown considerable progress, the expectation now being that the manufacturing of different electronic devices becomes feasible. The wide band-gap semiconductor SiC, with its excellent thermal conductivity, large breakdown fields, and resistance to chemical attack, will be the material of choice for these applications. Realized prototype power devices of SiC, like rectifier diodes, and junction field-effect transistors, show indeed encouraging performance results under extreme conditions (54)-(66). In the optical device arena, the ever increasing need for higher density optical storage and full color display technologies are driving researchers to develop wide band-gap semiconductor emitting technologies which are capable of shorter wavelength operation. Since the different energy gap values of SiC all happen to lie in the visible range of the spectrum, SiC is an interesting optical device material. Indeed, blue light emitting diodes were the first electronic SiC devices which found a good sale. Some SiC polytypes are in addition most promising as photodetective material sensitive to ultraviolet radiation. SiC is a good candidate for a short wave length diode laser. Prototype transistors have been fabricated from SiC, and the microwave and high temperature performance of SiC transistors have been studied. Devices like field effect transistors, bipolar storage capacitors, and ultraviolet detectors have been fabricated (57)-(64). SiC has a relatively high atomic bonding energy which is responsible for its mechanical strength and chemical stability at high temperatures. This material can without major difficulty, be crystallized in several polytypes, primarily due to similar geometric structures and atomic bonds (1)-(11). The different stacking of C-Si bilayers remarkably influences the properties of SiC. The most pronounced example concerns their electronic structure. Hence, a controlled epitaxial growth of different polytypes on each other would lead to high-quality heterostructures of chemical identical material with a locally adjustable band gap (7)-(14). Meanwhile, growth of heterocrystalline structures seems to be possible (4), but exhibits problems with the reproducibility and the crystal quality. Another possibility to create a combination of two polytypes is a solid-solid phase transition, which transforms one polytype into another one (6)-(8). However, polytypism also gives some advantages for constructing electronic devices, for example homo-material heterostructures. Quantum wells can be made by embedding a SiC polytype in another polytype with a wider gap(55)-(60). Among the SiC polytypes, 6H is most easily prepared and best studied, while the 3C and 4H polytypes are attracting more attention for their superior electronic properties. The very simple structure 2H is, in fact, very rarely produced by the employed growth techniques. Already, commercial applications have been done but most of the developments in industry

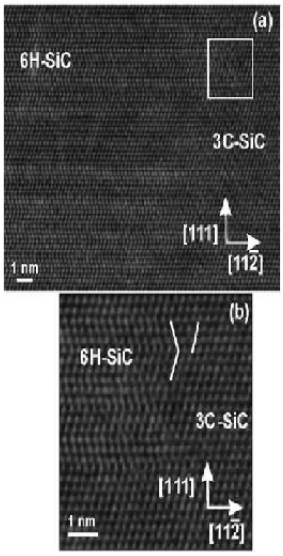

Fig. 1. (a) HRTEM image, displaying that the 3C/6H-SiC polytipic transformation takes place by three bilayers thin lamellae twinned along the (111) planes and bounded along the (11$\bar{2}$) planes. Image (b) presents a magnification of the area marked by the square in (a) (56).

and research laboratories focus on two hexagonal polytypes : the 6H and 4H-SiC varieties. The polytypism of SiC makes it non-trivial to grow single phase material, but it also offers some potential advantages if crystal growth methods can be developed sufficiently to capitalize on the possibility of polytype homo/heterojunctions (see figure 1).

2.1 Polytypism in SiC

SiC is a wide band gap semiconductor that can be synthesized in a variety of polytypes: polytypism, can be considered as a one dimensional variant of polymorphism (1)-(8). Indeed, while the term polymorphism generally refers to the possibility of an element or compound to crystallize in different structures, polytypes only differ for the stacking sequence of atomic layers along one crystalline direction. We include SiC in the group of polytypes because of its simplicity and the fact that its hexagonality is 100%. All various SiC-polytypes have the same stoichiometry and the same bonding configuration between next nearest neigbors. More than 200 polytypes of SiC exhibiting a wide range of properties have been reported (1). There are a lot of more complex polytypes in which the bonding arrangement (cubic vs. hexagonal) are repeated periodically. Due to that periodic repetition the SiC-polytypes are also called to be natural superlattices. However, only few of those polytypes are commonly found and those are relatively simple compared to the rest. The bandgaps differ widely among the polytypes ranging from 2.3 eV for 3C-SiC to 2.9 eV in 6H SiC to 3.3 eV for 2H SiC. In general, the greater the wurtzite component, the larger the bandgap.

A shorthand has been developed to catalogue the literally infinite number of possible polytype crystal structure. In this notation the number of layers in the stacking direction, before the sequence is repeated, is combined with the letter representing the Bravais lattice type: cubic

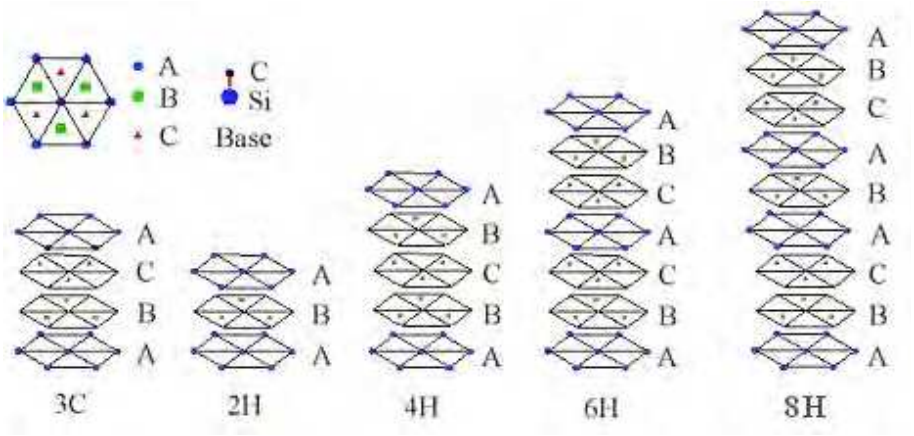

Fig. 2. Three-dimensional perspective views of the primitive hexagonal unit cells of the 3*C*-(zinc-blende), 2*H*-(wurtzite), 4*H*-, 6*H*-, and 8*H*-SiC polytypes. The stacking sequences ABC (3C), AB (2*H*), ABCB (4*H*), ABCACB (6*H*) and ABCAB ACB (8*H*) are also indicated.

(C) or hexagonal (H). With reference to figure 2, if the first Si-C layer is labelled A, the next layer that can be placed according to a closed packed structure will be placed either on B or C. The different polytypes are constructed by permutations of these three positions. In figure 2 the stacking sequence is shown for the most common polytypes, 3C, 2H, 4H, 6H, and 8H, which are very interesting for their technological applications. Three-dimensional perspective views of the primitive hexagonal unit cells of the 2H-, 3C-, 4H-, 6H-, and 8H-SiC polytypes. In the case of SiC, the basic units are tetrahedrons with a C(Si) atom at the center, surrounded by four Si(C) atoms covalently bonded: these units are periodically repeated in closed-packed hexagonal layers, whose stacking sequence gives rise to the different polytypes. Though being different in the long range order, the several polytypes show a similar local chemical environment for both the carbon and silicon species; in particular each Si(C) atom is situated above the center of a triangle of C(Si) atoms and underneath a C(Si) atom belonging to the next layer in a tetrahedral coordination. The SiC-polytypes consist of double silicon-carbon layers which are stacked on top of each other in the c-axis direction. A local arrangement of three consecutive double layers is called hexagonal, if it is like the arrangement of double layers in wurzite. It is called cubic, if the stacking arrangement is the same as for the zinc-blende structure. The basic structural elements is the SiC bilayer composed of one Si [0001] plane and the adjacent C[0001] plane. The SiC polytypes are differentiated by the stacking sequence of the tetrahedrally bonded SiC bilayers, such that the individual bond lengths and local atomic environments are nearly identical, while the overall symmetry of the crystal is determined by the stacking periodicity. Each SiC bilayer, while maintaining the tetrahedral bonding scheme of the crystal, can be situated in one of three possible positions with respect to the lattice. These are each arbitrarily assigned the notation A, B, or C. Depending on the stacking order, the bonding between Si and C atoms in adjacent bilayer planes is either of a zincblende (cubic) or wurtzite (hexagonal) nature. Zincblende bonds are rotated 60° with respect to nearest neighbors while hexagonal bonds are mirror images (Figure 2). Each type of bond provides a slightly altered atomic environment making some lattice sites inequivalent in polytypes with mixed bonding schemes and reducing the overall symmetry. These effects are important when considering the substitutional incorporation and electronic transport properties of

SiC. If the stacking is ABCABC..., the purely cubic, i.e., a zinc-blende structure consisting of two interpenetrating face-centered (fcc) cubic lattices. Zincblende structure commonly abbreviated as 3C SiC (or β-SiC) is realized (Figure 2). 3C SiC is the only possible cubic polytype. The stacking direction of the basal planes perpendicular to the planes is in fact [111] direction of the cubic unit cell of 3C-SiC as indicated in the figure. The family of hexagonal polytypes is collectively referred to as alpha SiC. The purely wurtzite ABAB... stacking sequence is denoted as 2H SiC reflecting its two bilayer stacking periodicity and hexagonal symmetry. All of the other polytypes are mixtures of the fundamental zincblende and wurtzite bonds. Some common hexagonal polytypes with more complex stacking sequences are 4H-, 6H- and 8H- SiC (Figure 2). Since the SiC polytypes are mixtures of cubic and hexagonal stackings, a quantity defined as the hexagonality H representing the fraction of hexagonal stackings out of all the stackings (cubic + hexagonal) in a polytype is used frequently to describe how much the polytype is cubic-like or hexagonal-like in structural sense [5]. As it is obvious from the definition, the hexagonality of 2H-SiC is 100 % and that of 3C-SiC is 0 %. It is naturally expected that a polytype with a smaller H should be closer to 3C, i.e., more cubic-like than one with a larger H in other material properties as well as in structure, and this is generally true for most of the polytypes. $4H-$, $8H-$SiC are composed equally of cubic and hexagonal bonds, while $6H-$SiC is two-thirds cubic. Despite the cubic elements, each has overall hexagonal symmetry. All these polytypes have higher periodicity (more Si-C bilayers) along the c-axis than 2H-SiC and they are in general called α-SiC together with 2H-SiC. 4H- and 6H-SiC are the most common polytypes, and single crystal wafers of these polytypes are currently available and hence all recent research for making commercial devices out of SiC are focused on these polytypes.

3. Empirical tight-binding model for hexagonal and n-hexagonal systems: General formalism of the tight-binding model for (0001) wurtzite:

The tight-binding approximation for band structure calculations uses atomic energy parameters and the expansion of the electron wave functions in terms of a linear combination of atomic orbitals (LCAO). In the LCAO method, the basic problem is to find the Hamiltonian matrix elements between the various basis states, as in the original paper of Slater and Koster (70); the matrix elements can be written for the basis functions sp^3 considering various possible interactions. In our recent calculations, a standard semi-empirical sp^3s^* tight-binding method (71) has been employed and the matrix elements are parametrized in order to reproduce the principal features to know the band structures.
The general form of the Hamiltonian is (72).

$$H(k) = \sum_{bb',l} \sum_{\alpha\beta} e^{ik.R^l_{bb'}} E^{bb'}_{\alpha\beta} \left(R^l_{bb'} \right) \tag{1}$$

where l labels the sublayers, b and b' refer to the atomic basis within a sublayer, and α and β are atomiclike orbitals. Given the $E^{bb'}_{\alpha\beta}$'s (bulk band structure) and the $\mathbf{R}^l_{bb'}$'s (SL geometry), we can construct the Hamiltonian matrix and diagonalize it directly for the eigensolutions.
In our recent study, we have performed a TB method with an sp^3s^* basis set (71). We used the nearest-neighbor TB parameters with a basis of five orbitals (s, p_x, p_y, p_z, and s^*) per atom. We have derived a TB Hamiltonian pH ($p = 2,4,6,8,..$) for different polytypes of SiC from the wz TB model. The label pH ($p = 2,4,6,8,..$) is the hexagonality for different polytypes. Consider a TB Hamiltonian of two different alternating wz crystals labelled "ca" in (0001)

direction, where c and a are labelled cation and anion atoms. The pH ($p = 2, 4, 6, 8,..$) contains $2(2n)$ atoms in a unit cell at R_i with five orbitals each; $|\alpha j >$, where α denotes the s, $x(= p_x)$, $y(= p_y)$, $z(= p_z)$ and s^*(=excited s) orbitals, and j represents the site index in a unit cell which runs from 1 through $2(2n)$.
For each wave vector $\mathbf{k}$ in the Brillouin zone (BZ), the Bloch functions can be constructed by the linear combination of atomic orbitals $|\xi, \mathbf{r}_\alpha, \mathbf{R}_l >$:

$$|\xi, r_\alpha, k >= \frac{1}{\sqrt{N}} \sum_l e^{ik.R_l + ik.r_\alpha} |\xi, r_\alpha, R_l > \tag{2}$$

Here ξ is a quantum number that runs over the basis orbitals s, s^*, p_x, p_y, and p_z on the different types of sites α in a unit cell. The N wave vectors $\mathbf{k}$ lie in the first BZ with the origin of the lth unit cell at $\mathbf{R}_l$, and $\mathbf{r}_\alpha$ represents the positions of the atoms in this unit cell.
The electronic eigen-states of the pH ($p = 2, 4, 6, 8,..$) are expanded as :

$$\begin{aligned} |k, \lambda > &= \sum_{\xi,\alpha} < \xi, r_\alpha, k | k, \lambda > |\xi, r_\alpha, k > \\ &= \sum_{\xi,\alpha} C_{\xi\alpha}(k, \lambda) |\xi, r_\alpha, k > \end{aligned} \tag{3}$$

λ denotes the band index and $C_{\xi\alpha}(\mathbf{k}, \lambda)$ is the eigen-wavefunction, which can be obtained by solving the Schrödinger equation.

$$\sum_{\xi,\alpha'} \left[\langle \xi, r_\alpha, k | H | \xi', r_{\alpha'}, k \rangle - E_\lambda(k) \delta_{\xi\xi'} \delta_{\alpha\alpha'} \right] < \xi, r_\alpha, k | k, \lambda >= 0 \tag{4}$$

Therefore, we obtain the Hamiltonian matrix for pH ($p = 2, 4, 6, 8,..$).

$$H = \begin{array}{c} \\ 1 \\ 2 \\ 3 \\ 4 \\ \\ \\ \\ n-1 \\ n \\ 1 \\ 2 \\ . \\ n-1 \\ n \end{array} \begin{array}{c} \begin{array}{cccccccccccccc} 1 & 2 & 3 & . & . & n-1 & n & 1 & 2 & 3 & . & . & n \end{array} \\ \begin{bmatrix} Ha & Hac & & & & & & & & & & & H_0^+ ca \\ Hc & H_0 ac & & & & & & & & & & & \\ & Ha & & & & & & & & & & & \\ & & Hc & & & & & & & & & & \\ & & & . & & & & & & & & & \\ & & & & . & & & & & & & & \\ & & & & & . & & & & & & & \\ & & & & & Ha & & & & & & & \\ & & & & & Hc & H_0 ac & & & & & & \\ & & & & & & Ha & Hac & & & & & \\ & & & & & & & Hc & H_0 ac & & & & \\ & & & & & & & & . & . & & & \\ & & & & & & & & & Ha & Hac & & \\ & & & & & & & & & & Hc & & \end{bmatrix} \end{array} \tag{5}$$

Here, the blocks $H_{c(a)}$, H_{ac}, and H_{0ac} denote intra-material interactions for pH ($p = 2, 4, 6, 8,..$), and every element represents a 5x5 matrix. The blocks H_{ca} and H_{0ca} are expressed as:

$$H_{ac} = \begin{bmatrix} a & ac \\ ac^+ & c \end{bmatrix}, \; H_{0ac} = \begin{bmatrix} aa & ac \\ ca & cc \end{bmatrix} \tag{6}$$

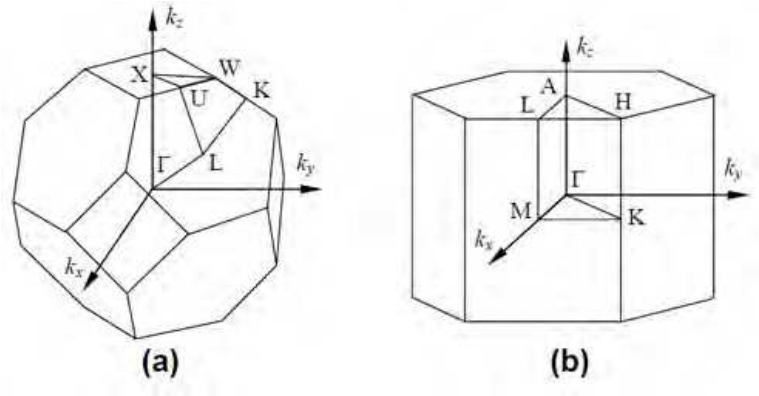

Fig. 3. Brillouin zones of (a) cubic (b) hexagonal structures.

The diagonal elements $H(j = a$, and $c)$ correspond to intra-site energies, and the others contain the nearest atomic interactions in the same layer (H_{ij}) or between two neighbor layers (H_{0ij}) perpendicular to the (0001) direction. The terms a and c are regarded as the anion and cation atoms of the SiC semiconductor. The intra-material elements in the Hamiltonian can be formed uniquely by using the corresponding bulk parameters. Our TB parameters (62) give the correct indirect and direct gap in comparison with Ref.(73) and are checked for their transferability to all considered structures by calculating the optoelectronic properties of different polytypes of SiC. This method reduces the size of the Hamiltonian matrix considerably compared with methods based on plane-wave basis and allows us to treat localized states. Our TB Hamiltonian can be generalized to the wz based SL's in (0001) direction with two different compounds and is efficient when extended it to investigate the electronic properties of wz SL's. Then, we present some of our recent results which we have obtained by our TB model for electronic and optical properties of SiC polytypes.

4. Electronic and optical properties of polytypic SiC

We start this section with some of our recent results for SiC polytypes in order to illustrate the electronic and optical properties of this system. With a TB scheme, the detailed calculations of electronic structure and optical properties of different polytypes of SiC are presented.

4.1 Electronic band structures of 3C-, 2H-, 4H-, 6H-, and 8H-SiC:

A very important aspect of the polytypism of SiC is the change in energy band structure, and how it does appear in the different polytypes. Having established the geometric structure for the polytypes, the electronic band structure was calculated along the symmetry directions (62). Figure 3 shows the BZs of cubic, and hexagonal polytypes with high symmetry points marked. The labeling of the symmetry points and the three symmetry lines out from the Γ point in the relevant hexagonal Bzs are shown in Figure 3.

The corresponding band structure of 3C-SiC is shown in figure 4. The conduction band minimum (CBM) for 3C-SiC is lying at the X point and the number of CBMs equals to three (2). The resulting TB band structures of SiC polytypes (2H, 4H, 6H, and 8H) are also represented in Figure 4 versus high-symmetry lines A-L-M-Γ-A-H-K-Γ. For all polytypes the gap is systematically identified as an indirect one. The valence band maximum is located for

all polytypes at the centre of the BZ. The valence band maximum (VBM) is found to be at the center of the BZ at Γ point for all polytypes. The zero energy is used for all polytypes. In the case of 2H-SiC, the CBM is at the K point with two equivalent CBMs (73), (74), (75), (77), while 4HSiC has its CBM at the M point giving three equivalent CBMs (22), (25),(76), (78),(79) [Figure 4]. For 6H-SiC, the theoretical calculations predict the conduction band supplying the global CBM to be very flat along the ML line and the CBM resides at some place on the line, resulting in six equivalent CBMs (22), (25), (78),(79). This has been confirmed experimentally from the Raman scattering measurement by Colwell et al. (80). However, the exact location of the CBM and the detailed shape of conduction band affecting the determination of effective electron mass are not yet well-established, either experimentally or theoretically. There are similarities between the band structures of the hexagonal polytypes, both in the valence and the conduction bands, especially between 4H, 6H and 8H-SiC structures. A significant difference between 2H and the other three hexagonal polytyes is that in 2H-SiC the two lowest conduction bands have an intersection along MK line and that the lowest band at K point has a one-dimensional representation (in the single group representation). Both in 4H, 6H and 8H-SiC the two lowest conduction bands at K point are degenerate. The intersection in 2H-SiC makes it possible for the second lowest band at the M point to provide a global conduction band minimum at the K point with C_{3v} symmetry whereas the minimum for 4H-SiC is at M (C_{2v}) and for 6H-, and 8H-SiC along the ML line (also C_{2v} symmetry), 44 % out from M towards L. The variation in band energy gaps is coming from the different locations of CBMs. This is related with the stacking and period of each polytype. Interestingly, it is predicted theoretically that the offsets of VBMs among different polytypes are quite small, at most 0.10-0.13 eV for the case of 2H and 3C (11),(14). In other words, the VBMs of all polytypes are similarly located in energy. This means that the considerable variation of band gap for different polytypes is mainly due to the difference of CBM location.

Another interesting point to note in the conduction band structures of SiC polytypes is the location of second CBM. According to the calculation done by Persson et al. (26),(38), the second CBM of 3C-SiC is at the same symmetry point (X) as the first one with 2.92 eV higher in energy and this was confirmed experimentally from optical absorption measurements with slightly larger energy difference (3.1 eV) between the two minima (13). Persson et al. calculations also show that the three hexagonal polytypes (2H, 4H, 6H) have their second CBMs located at the M point and the energy difference between the first and second CBMs is 0.60 eV for 2H, 0.122 eV for 4H, and 1.16 eV for 6H respectively. The energy position of the second CBM in 4H-SiC has been probed experimentally by BEEM (56)-(58) and optical phonon spectra measurements (59)-(63), with measured energy that ranges 0.10-0.14 eV above the first CBM. The band gaps of several common polytypes of SiC have been measured carefully by Choyke et al. from the optical absorption or luminescence spectra of the polytypes (27). The measured band gaps range widely from 2.390 eV for 3C-SiC to 3.330 eV for 2H-SiC and lot of work has been done to understand all details of the corresponding variations. Those for 4H- and 6H-SiC which are in between the two extreme cases in structure are measured to be 3.265 eV and 3.023 eV respectively. So, from fig.4, it is clear that the valence and the conduction bands are well described. Moreover, our results are in good agreement with the experimental results (74). All energies are with reference to the top of the valence band. The results show that SiC is an indirect gap semiconductor. In addition, the calculated energy gaps of SiC are in good agreement with the other results (73), (74), (75), (77).

Values of lowest indirect forbidden gaps (E_g) are listed in Table 1 in comparison with the available data in the literature and experimental results. Our TB model provides good results

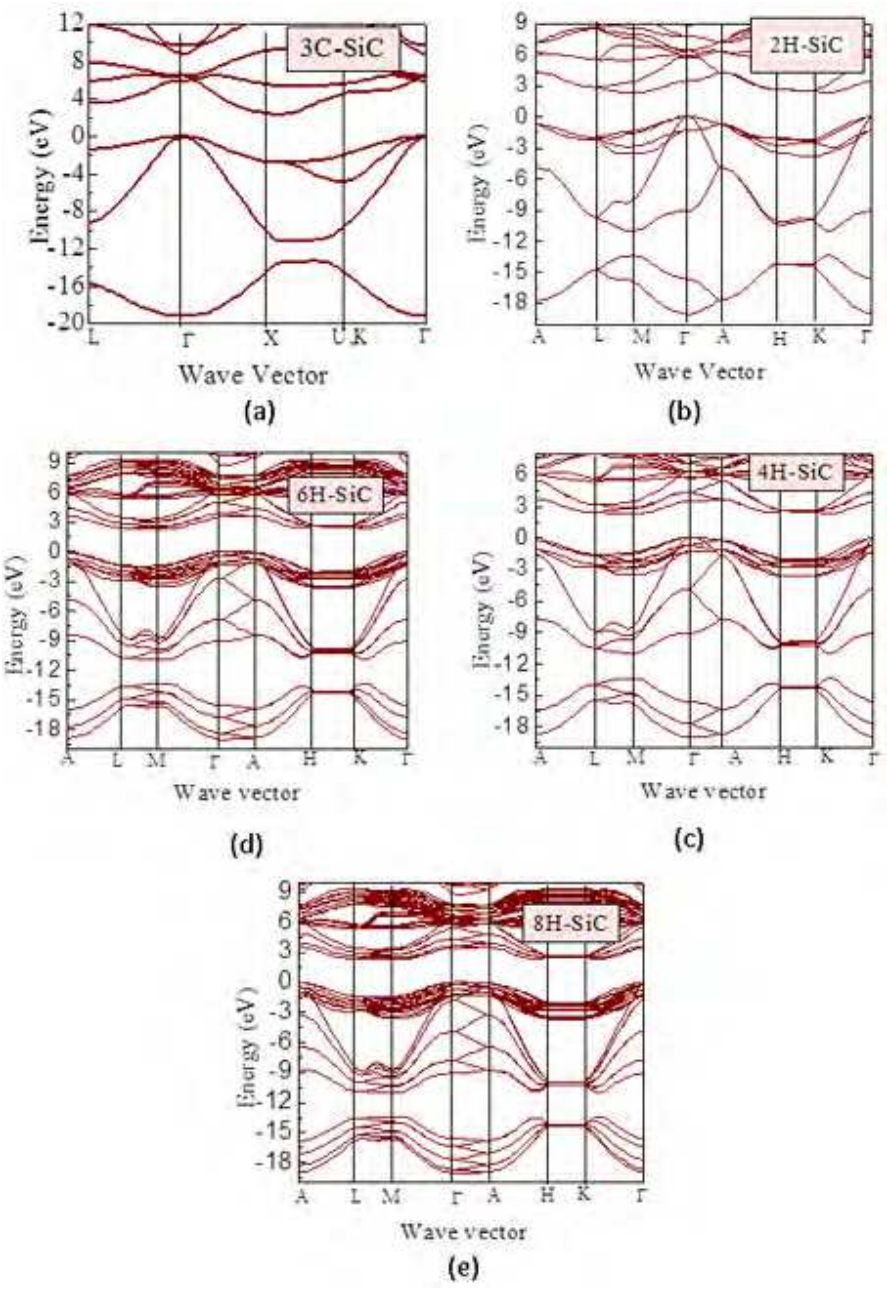

Fig. 4. Band structures for 3C-, 2H-, 4H-, 6H-, and 8H-SiC calculated by our sp^3s^* TB model (62).

	This work	Experiement	GW	LDA+U	GGA/LDA	EPM	ETB	NTB
3C	2.389	2.39[c]	2.38[b]	2.52[d]	1.5[e], 1.27[f]	2.30[g]	2.47[h]	1.33[i]
2H	3.33	3.30[a]	3.31[b]	3.33[d]	2.10[f]			
4H	3.20	3.19[a]	3.18[b]	3.16[d]	2.57[e], 2.18[f]	3.20[g]		
6H	2.86	2.85[a]	2.84[b]	2.90[d]	2.28[e], 1.96[f]	2.99[g]		
8H	2.86	2.86[a]	2.84[b]					

Table 1. Values of indirect gap of SiC polytypes (62).
[a] Experimental data (75)
[b] GW calculations (73)
[c] Experimental data(74)
[d] LMTO calculations (78)
[e] GGA calculations (79)
[f] LDA calculations (25)
[g] EPM calculations (22)
[h] ETB values (76)
[i] NTB values (77)

which agree with other calculations (22), (25), (73), (75), (76), (77), (78),(79) and experimental data (74). The general findings that all considered polytypes are indirect semiconductors are not surprising, including that the conduction-band minimum is located at X point in the zinc-blende structure or at M in the hexagonal BZ of 2H. Diamond and silicon show a similar behavior, there the conduction-band minima are situated on the ΓX line near X [110]. The *X* point in the fcc BZ represents the position of the minimum in the zinc-blende 3C-SiC. Two of these X points are folded onto M points of the hexagonal BZ of the corresponding 2H structure. The exact positions depend on the details of the calculations, the ratio c/a of the hexagonal lattice constants, as well as the atomic positions within the hexagonal unit cells. Moreover, the upper valence band has the lowest energy in X, so that the repulsive interaction between the lowest conduction band and the highest valence band should be small. In the wurtzite structure, the situation is changed. First of all, the zinc-blende X is folded onto 2/3LM in the hexagonal BZ of 2H. This point has a lower symmetry and the bonding and antibonding combinations of the C 2s orbital and a Si 3p orbital, of which the state mainly consists, can interact with more closer lying states. The minimum at K point, that has a similar orbital character as the states at the zinc blende W point, gives rise to the lowest empty band. The energetical distance of the valence and conduction bands in K point is remarkably reduced. The resulting stronger interaction pushes the conduction-band minimum away from the valence bands. States on the LM line near M point form the lowest conduction-band minimum. Surely, the minimum in the wurtzite structure 2H-SiC is located at the **k** point in the center of the BZ edge parallel to the *c* axis similarly to hexagonal diamond (79). We find the conduction band minima at M point for 4H and, respectively, at about 0.63LM for 6H and 8H. This result is somewhat surprising since the fcc X point should map onto 1/3LM for 4H and M for 6H and 8H. That means that the simplifying folding argument is not exactly valid going from one polytype to another one. The actual arrangement of atoms and bonds in the unit cells gives rise to changes in the band positions and dispersion. The exact minimum position is particularly sensitive to the details of the atomic structure since the lowest conduction band between L and M is rather flat. This flatness increases with the lowering of the LM distance in k space. Increasing the period of the superstructure along the optical axis (line Γ-A in the BZ) causes band folding, which can be seen for the Γ-A and K-H

directions for the SiC polytypes shown in Figure 4. The overall features of the band structures agree well with previous calculations . Differences concern the magnitudes of the various band gaps, where the effect is related to the variations in the position of the conduction-band minima. An interesting problem concerns the preparation of heterostructures on the base of chemically identical, but structural inequivalent semiconductors, more strictly speaking of different polytypes. The key parameters of such structures are the band offsets at the interface.

4.2 Effective masses of 3C-, 2H-, 4H-, 6H-, and 8H-SiC

The effective electron masses for the different polytypes have been calculated and measured experimentally by different scientific groups (19), (22), (26), (81), (82), (83). The values vary depending on the experimental techniques or model used, especially for the hexagonal polytypes. Results for the lowest conduction band minima in K, M points, or at the LM line near M point are calculated (62). For electrons we give the full inverse effective-mass tensor along the principal axis determined by the c axis of the structure and the position of the minimum in $\mathbf{k}$ space. We consider the longitudinal masses $m_{||}$ parallel to the connection line between the minimum position and more strictly speaking parallel $M\Gamma(4H)$, $K\Gamma$ $(2H)$ and $(LM)\Gamma$ $(6H, 8H)$. The two transverse masses $m_{\perp 1}$, $m_{\perp 2}$ are distinguished according to the anisotropy of the system. $m_{\perp}$ denotes the transverse mass parallel to the c axis. In the calculation of $m_{\perp 1}$ we use the direction ML. For the estimation of the second transverse mass $m_{\perp 2}$ of the hexagonal polytypes we replace the correct direction by the line MK in an approximate manner.

Our previously calculated values of the electron effective masses in three principal directions with the tight-binding method (62) are presented in table 2 in comparison with other theoretical and experimental data. All values of the electron effective masses agree with experimental values, when available, and for 3C-, 2H-, and 4H-SiC, our results agree with the majority of earlier calculations (22). We report in the same table our values of m^* for $8H$-SiC. There is no available experimental data for comparison. No clear trend with the hexagonality or the extent of the unit cell can be derived from table 2 for the electron masses. This is not astonishing since the conduction band minima appear at different $\mathbf{k}$ points in the BZ. Only in $4H$ case one observes the minimum at the same point M. A remarkable anisotropy of the electron effective mass tensor is found for $6H$ and $4H$. In space directions (nearly) parallel to $M\Gamma$ and $L\Gamma$ heavy electrons appear whereas the mass for the electron motion in the plane perpendicular to c axis but parallel to the edge MK of the hexagonal BZ is small. This is a consequence of the flatness of the lowest conduction bands in the most space directions. The electron-mass anisotropy in the $2H$ polytypes at M or K is much smaller. The findings for the conduction band masses have consequences for the electron mobility, since this property is proportional to the inverse mass. We expect that at least for the mostly available $6H-$ and $4H$-SiC polytype, the current directions should be carefully selected. Otherwise, too small electron mobilities result. 2H-SiC have more parabolic behavior around their minima, whereas in 4H- and 6H-SiC the interaction between the two close-lying bands at the M point will affect the parabolicity, especially for the flat curvatures in the c direction. The best agreement between theory and experiment seems to be for the 2H-SiC pure hexagonal polytype and the 3C-SiC cubic polytype. For the 8H-SiC polytype there are not yet any experimental results for the effective electron masses. Also there is only one experimental report for the longitude effective mass of 6H-SiC. For the hole effective masses there are few theoretical reports of the polytypes and even fewer are the experimental values. The effective electron masses of 3C- and 4H-SiC have been measured experimentally and

Mass	3C	2H	4H	6H	8H
$m_{\parallel}$	0.69	0.40	0.60	0.65	0.67
	0.667[c]	0.42[a]	0.58[a]	0.68[a]	
	0.70[b]	0.43[f]	0.53[b]	0.44[b]	
	0.449[d]		0.58[e]	0.77[e]	
	0.68[f]		0.57[f]	0.75[f]	
$m_{\perp 1}$	0.25	0.24	0.36	1.19	1.38
	0.247[c]	0.22[a]	0.33[a]	1.25[a]	
	0.24[b]	0.26[f]	0.31[e]	1.14[b]	
	0.23[f]		0.31[f]	1.42[e]	
				1.83[f]	
$m_{\perp 2}$	0.25	0.40	0.21	0.10	0.15
	0.247[c]	0.42[a]	0.29[a]	0.13[a]	
	0.24[b]	0.43[f]	0.19[b]	0.43[e]	
	0.23[f]		0.28[e]	0.24[f]	
			0.28[f]		

Table 2. Effective masses of electrons in the conduction-band-minima. All values in units of the free-electron mass m_0 (62).

[a] Experimental values (81).
[b] EPM calculations (22).
[c] Experimental values (82).
[d] LMTO (GW) (83).
[e] LMTO (19).
[f] FPLAPW (26).

reported by several groups, and they agree quite well with the theoretically calculated values (19), (26), (83). For 6H-SiC, only the longitudinal effective mass along the c-axis has been measured (82), but due to the peculiar band shape along the direction there is still a large inconsistency between the measured value and the calculated ones, even among the values calculated theoretically by different groups (19), (26), (83). However, only the hole effective masses of 4H-SiC have been measured experimentally and reported by Son et al. (81).

4.3 Total density of states of 3C-, 2H-, 4H-, 6H-, and 8H-SiC

We have applied the tetrahedron technique directly from the eigenvalues and the angular momentum character of each state. This is done by dividing up the Brillouin zone into 48 tetrahedron cube. The total density of states (TDOS) of 3C-SiC, corresponding to the band structure is given in figure 5 (62). The 3C-SiC have valence band density of states qualitatively similar to homopolar semiconductors, except for the gap which opens at X point. This gap is related to different potential for the cation and anion potentials. This "antisymetric" gap has been proposed as a measure of crystal ionicity. The lowest states contain a low-lying C s-derived band about 17 eV below the VBM. The lowest states of the VB from -17 to -13 eV has primarily s character and is localized on the anion. The large peak at -10 to -7 eV comes primarily from the onset of the second valence band at points X and L. The states of this band is primarily of cation s character, it changes rapidly to anion p-like at the top of valence band. From the Fig 5, it is apparent that there is a significant amount of Si p hybridization all the way up to the VBM. A comparison with the corresponding DOS curve of the experimental

results reveals excellent agreement for energies below 4 eV. The bandwidths and energies are in good agreement with photoemission results (74).
The DOS was determined by the tetrahedron integration over a mesh that was generated by six cuts in the Γ-M direction of the BZ and included 112, 84, 78 and 56 points in the irreducible part of 2H, 4H, 6H and 8H BZ, respectively. In Figure 5 total densities of states of SiC polytypes (62) are shown which can be used for the interpretation of photoemission spectra of SiC. The lowest valence band in 6H SiC between -19.0 and -13.0 eV is dominated by *s*-electrons of C atom. The maximum at 14.85 eV in the total DOS is dominated by the *s*-electron of Si. The upper part of the valence band of 6*H* SiC is dominated mainly by the *p*-electron of C and Si. The conduction band is mainly dominated by the *s*, and *p*-electrons of Si, whereas *p*-electrons of C are less dominant. There is a noticeable difference of the p-state occupation for different polytypes and for different sites in the same polytype. The band width of the valence band agrees with previous works represented in many literatures [(22), (25), (73), (75), (77), (78)], where 18.0 eV were obtained. Our value of the valence band width (≈19.0 eV) of 6*H* SiC is lower than in cubic SiC as expected (25), (73),(78),(79).
In the figure 5, one can see that the valence band, as expected, consists of two subbands. The energy width of these subbands and the total bandwidth are very similar for the four polytypes. In α-SiC polytypes the lower-lying subbands is in the range from about -19.5 to -13 eV and is dominated by the atomic Si 3s+3p states and the localized atomic C 2s states, whereas the higher subband also consists of Si 3p and 2p states. In the higher subband the Si 3s and C 2p states dominate at lower energies and the C 2p states dominate at higher energies. Even if it is not straightforward to compare photoemission spectra with the DOS, the clear peak at about -11.1 eV, arising from the atomic C 2p and Si 3s states, can probably be identified with the experimental value -10.5 eV (74). Also, the total band-width and the width of the higher subband seem to be in agreement with experimental results. The calculated width of the total band (higher subband) is about 8.5 eV for all four polytypes, whereas the experimental results for α-SiC polytypes are about 10.0 eV (74).
Since band structures accurate close to the band gap are desired, it is useful to examine the density of states in this region. As found experimentally (74) and theoretically (25), (73),(78),(79), the major differences between the density of states of the individual SiC polytypes calculated with our TB model band structure is in the conduction bands. The results are compared with results from density-functional theory (DFT) (75). Both results of 2H-, 4H-, 6H-, and 8H-SiC show not only an increasing band gap, but an increase in the steepness of the rise in the density of states at the conduction band edge with increasing hexagonality.

4.4 Optical absorption of 3C-, 2H-, 4H-, 6H-, and 8H-SiC:

Many optical properties, such as the dielectric function, the reflectivity, absorption, etc.., are related to the band structure of cristalline solids. Most of them can be derived from the dielectric function which is measured directly and reliably by spectroscopy ellipsometry. It is worth calculating the optical absorption for different polytypes of SiC. Theoretically, the spectra are seen to be dependent on quantities such as density of states and matrix elements coupling the initial to final state. In the case of absorption spectra for bulk semiconductors, the main structures are observed to be correlated with the inter-band critical points. It is very common to assume that the dipole matrix elements involved are constant throughout the Brillouin zone and to compare the spectra directly with joint density of states (48).
We can compute the matrix elements starting from an empirical Hamiltonian even if the full wave functions are not known. The Slater-Koster method is computationally very economical

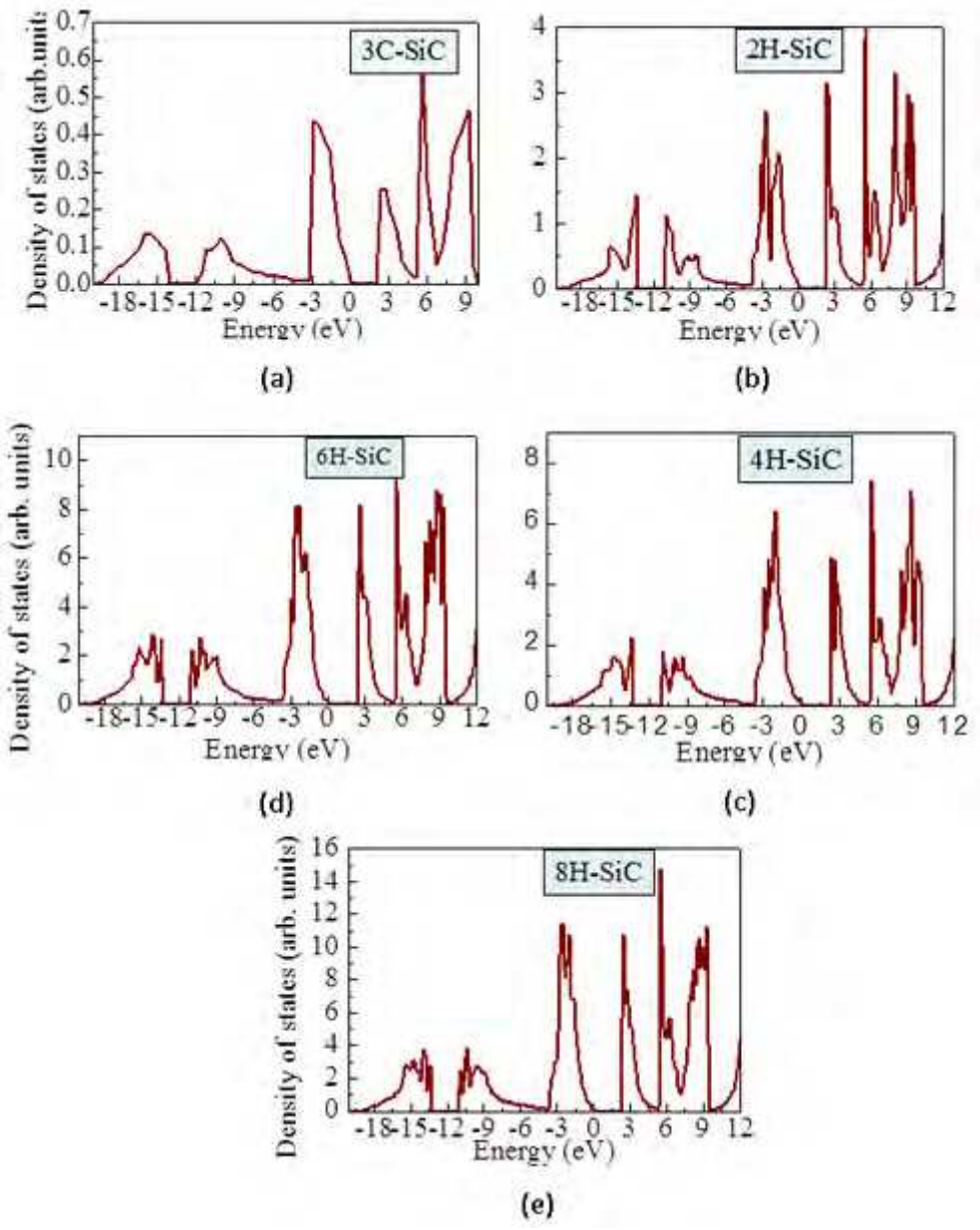

Fig. 5. Density of states for the 3C-, 2H-, 4H-, 6H-, and 8H-SiC polytypes (62).

in obtaining the full-zone band structure of semiconductors, and our procedure for the optical matrix elements requires little additional computation beyond solving the eigenvalue problem for the energies.

4.4.1 Applications of optical matrix elements:

Optical-absorption spectra in semiconductors are normally dominated by transitions from the valence to the conduction bands. Then, it is possible to compute the joint density of states (JDOS) for SiC polytypes that is given by the below formula. The purpose is to see how our TB calculations are extended to optical properties.

$$J(E) = \Omega \sum_{cv} \int_{FBZ} \frac{d^3k}{(2\pi)^3} \delta\left(E_{cv}(k) - \hbar\omega\right) \tag{7}$$

where Ω is the real-space unit-cell volume.
where $E_{cv} = E_c(k) - E_v(k)$ for the JDOS per component (48).
We have computed the JDOS for SiC polytypes (62), hence, the interband transitions in Eq.(7) are all of the valence-conduction type. The interest in the JDOS lies in the fact that the momentum matrix elements are assumed constant over the Brillouin zone. The band summations in Eq.(7) involve all states in the valence band and lowest states in the conduction band. The summations in Eq.(7) are over special points in the Brillouin zone. In our calculations, we took 32, 28, 24, 20 special **k**-points for 2H, 4H, 6H and 8H respectively in the Brillouin zone (21).

4.4.2 Joint density of states of 3C-, 2H-, 4H-, 6H-, and 8H-SiC:

Before discussing the effect of the optical transition matrix elements, we consider the JDOS (see figure 6). In order to get more information on the interband transition, we present our recent calculated joint density of states for SiC polytypes (62). We have determined the transition responsible for the major contributions to these structures. This was done by finding the energy of the desired peak or shoulder on the joint density of states graph and then examining the contribution to joint density of states at that energy from the constituent interband transitions. The fundamental gap is well understood and is attributed to $\Gamma_{15} \rightarrow X_1$transition in 3C-SiC. We examine a large peak associated to $\Gamma_{15} \rightarrow L_1$ transition which occurs at 3.8 eV. The second major peak in JDOS, comes from the transition $\Gamma_{15} \rightarrow \Gamma_1$ which occurs at 5.2 eV. However, our band structure is satisfactory with respect to these transitions. The principal behavior of the joint density of states is very similar for the various 2H-, 4H-, 6H-, 8H- polytypes considered. The two peaks below the ionic gap exhibit a different behavior with the number n of SiC bilayers in the unit cell. Whereas that at higher energy around 7 eV is rather independent of the polytype, the low-energy peak around 8 eV is broadened with rising number n. We relate this fact to the folding effect parallel to the c axis. It causes an opposite variation of the band curvature along the LM and HK lines in the hexagonal BZ (25), (73), (78). The intensity of the two most pronounced peaks at 3.5 and 2.1 eV in the region of the upper valence bands monotonically follow the hexagonality of the structures (25), (75), (78),(79). Strong contributions to these peaks also arise from the LM line. The most drastic change in the conduction band region occurs near the onset of the density of states. Its steepness over several eV again follows the hexagonality of the polytype. The particular shape of the onset however depends on the number of bilayers and therefore on the folding effect as already has been pointed out by Lee et al. (84). The consequences can be clearly seen in the joint density of states. Their low-energy tails increase with decreasing hexagonality.

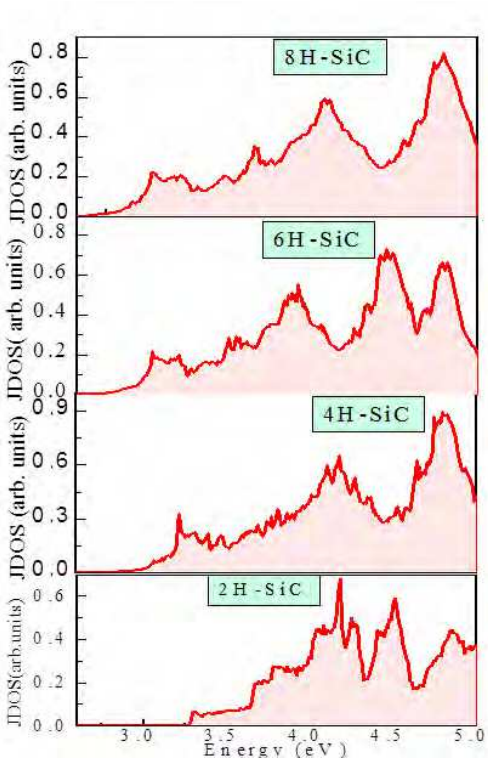

Fig. 6. Joint density of states for the 3C-, 2H-, 4H-, 6H-, and 8H-SiC polytypes (62).

5. Summary and conclusions

This chapter reviewed the general aspects of the optical properties as well as the electronic structures of SiC indirect-band-gap semiconductor polytypes. We presented our recent results of the band structures, the total densities of states, and the optical absorption of different polytypes of SiC using the empirical tight-binding approximation. The set of TB parameters is transferable to all hexagonal 2H-, 4H-, 6H-, and 8H-SiC structures. We illustrated how the tight-binding formalism can be used to accurately compute the electronic states in semiconductor hexagonal polytypes. This approximation is known to yield a sufficiently accurate conduction band and to give its minimum position correctly. To this end we have presented our new developed tight-binding model which carefully reproduces ab initio calculations and experimental results of SiC polytypes. It is likely that our TB approach could be applied to SiC polytypes with even larger unit cells than 8*H* using the variation in band gap with hexagonality in cases where experimental band gaps are undetermined. SiC system exhibits rather interesting features which differ greatly from those other semiconductor compounds with respect to optical properties as well as in electronic structure. We refer to this aspect of superperiodicity that is the possibility of modifying the optical properties of the material. Furthermore, the interband optical matrix elements can be tailored. It has been shown that our recent results indicate that our TB calculations are suitable for describing optical properties in more complex polar semi-conductors. In addition, the optical properties

suggest that the hexagonal SiC polytypes composed of an indirect-band-gap semiconductors offer a great potential for application to optical devices.

6. References

[1] A. P Verma and P. Krishna, Polymorphism and Polytypism in Crystals, (Wiley, New York, 1966).
[2] W. J. Choyke, in *The Physics and Chemistry of Carbides, Nitrides and Borides,* NATO ASI Ser., Ser. E, Appl. Sci. Vol. **185**, R Freer, Ed. (Kluver, Dordrecht, 1990), p. 563.
[3] K. Karch, G. Wellenhofer, P. Pavone, U. Röβler, and D. Strauch, *Structural and Electronic Properties of SiC polytypes*, in Proceeding of 22nd International Conference On the Physics of Semiconductors, Vancouver, 1994.
[4] R. F. Davis, Z. Sitar, B. E. Williams, H. S. Kong, H. J. Kim, J. W. Palmour, J. A. Edmond, J. Ryu, J. T. Glass, and C. H. Carter, Jr. Mater. Sci. Eng B **1**, 77 (1988).
[5] N. W. Jepps and T. F. Page, Progr. Cryst. Growth Charact. 7, 259 (1983).
[6] Diamond, SiC and Nitride Wide Bandgap Semiconductors, edited by C. H. Carter. Jr., et al. (Materials Research Society, Pittsburgh, 1994).
[7] P. Y. Yu, M. Cardona, Fundamentals of Semiconductors ï£¡ Physics and Material properties, Spinger (2005).
[8] Silicon Carbide, III-Nitrides and Related Materials, edited by G. Pensl, H. Morkoï£¡, B. Monemar, and E. Janzï£¡n (Trans Tech publications, Switzerland, 1998).
[9] D. B. Holt, B. G. Yacobi, ï£¡Extended Defects in Semiconductors. Electronic Properties, Device Effects and Structuresï£¡, Cambridge University Press (2007).
[10] V. I. Gavrilenko, A. V. Postnikov, N. I. Klyui, and V. G. Litovchenko, Phys. Stat. Sol. B **162**, 447 (1990).
[11] M. S. Miao, S. Limpijumnong, and W. R. L. Lambrecht, Appl. Phys. Lett. 79, 4360 (2001).
[12] Walter R. L. Lambrecht and M. S. Miao, Phys. Rev. B 73, 155312 (2006).
[13] C. Tivarus, J.P. Pelz, M.K. Hudait, S.A. Ringel, Appl. Phys. Lett. 87 182105 (2005).
[14] K. J. Russell, Ian Appelbaum, and V. Narayanamurti, Phys. Rev. B 71, 121311(R) (2005).
[15] W. R. L . Lambrecht, and B. Segall, Phys. Rev. B41, 2832 (1990).
[16] K. Karch, G. Wellenhofer, P. Pavone, U. Röβler, and D. Strauch, Structural and Electronic Properties of SiC polytypes, in Proceeding of 22nd International Conference On the Physics of Semiconductors, Vancouver, 1994.
[17] J. Bernholc, A; Antonelli, C. Wang, and R. F. Davis, in *Proceedings of the Fifteenth International Conference on Defects in Semiconductors*, Budapest, 1998.
[18] W. R. L. Lambrecht, B. Segall, M. Methfessel, and M. van Schilfgaarde, Phys. Rev. B **44**, 3685 (1991).
[19] W. R. L. Lambrecht, S. Limpijumnong, S. N. Rashkeev, and B. Segall, Phys. Stat. Sol. (b) 202, 5 (1997).
[20] W. van Haeringen, P. A. Bobbert, and W. H. Backes, Phys. Stat. Sol. (b) 202, 63 (1997).
[21] B. Adolph et al., Phys. Rev. B **55**, 1422 (1997).
[22] G. Pennington and N. Goldsman, Phys. Rev. B 64, 45104 (2001).
[23] A. Bauer, Phys. Rev. B 57, 2647 (1998).
[24] C. Person, and U. Lindefelt, J. Appl. Phys. 82, 5496 (1997).
[25] P. Kï£¡ckell, B. Wenzien, and F. Bechstedt, Phys. Rev. B 50, 10761 (1994).
[26] C. Persson and U. Lindefelt, J. Appl. Phys. 82, 5496(1997).
[27] W. J. Choyke, D. R. Hamilton, and Lyle Patrick, Phys. Rev. 133, 1163 (1964).
[28] Lyle Patrick, D. R. Hamilton, and W. J. Choyke, Phys. Rev. 143, 526 (1994).

[29] A. O. Konstantinov and H. Bleichner, Appl. Phys. Lett. 71, 3700 (1997).
[30] H. Lendenmann, F. Dahlquist, N. Johansson, R. Sonderholm, P. A. Nilsson, J. P. Bergman, and P. Skytt, Mater. Sci. Forum 353-356, 727 (2001).
[31] R. S. Okojie, M. Zhang, P. Pirouz, S. Tumakha, G. Jessen, and L. J. Brillson, Appl. Phys. Lett. 79, 3056 (2001); Mater. Sci. Forum 389-393, 451 (2002).
[32] L. J. Brillson, S. Tumakha, G. Jessen, R. S. Okojie, M. Zhang, and P. Pirouz, Appl. Phys. Lett. 81, 2785 (2002).
[33] H. Iwata, U. Lindefelt, S. ï£¡berg, and P. R. Briddon, Mater. Sci. Forum 389-393, 439 (2002); J. Appl. Phys. 93, 1577 (2003).
[34] P. Pirouz, M. Zhang, J.-L. Demenet, and H. M. Hobgood, J. Appl. Phys. 93, 3279 (2003).
[35] A. Galeckas, J. Linnros, and P. Pirouz, Appl. Phys. Lett. 81, 883 (2002).
[36] A. T. Blumenau, C. J. Fall, R. Jones, S. ï£¡berg, T. Frauenheim, and P. R. Briddon, Phys. Rev. B 68, 174108 (2003).
[37] A. T. Blumenau, R. Jones, S. ï£¡berg, and T. Frauenheim, Mater. Sci. Forum 457- 460, 453 (2004).
[38] P. O. A. Persson, L. Hultman, H. Jacobson, J. P. Bergman, E. Janzï£¡n, J. M. Molina-Aldareguia, W. J. Clegg, and T. Tuomi, Appl. Phys. Lett. 80, 4852 (2002).
[39] H.P. Iwata, U. Lindefelt, S. ï£¡berg, P.R. Briddon, Phys. Rev. B, Vol. 65 (2001).
[40] H.P. Iwata, U. Lindefelt, S. ï£¡berg, P.R. Briddon, J. Phys. Condens. Matter Vol.14 p. 12733, (2002).
[41] H.P. Iwata, U. Lindefelt, S. ï£¡berg, P.R. Briddon, Physica B, 340-342 p.165, (2003).
[42] H.P. Iwata, U. Lindefelt, S. ï£¡berg, P.R. Briddon, Microelectronics J. 34 371 (2003).
[43] J. Camassel, S. Juillaguet, J. Phys. D: Appl.Phys. 40, 6264 (2007)
[44] A. Chen, P. Srichaikul, Phys. Stat. Sol. B202, 81(1997).
[45] W.Y. Ching et al., Mater. Sci. And Eng. A 422, 147-156 (2006).
[46] A. Galeckas, J. Linnros, B. Breitholtz, H. Bleichner, J. Appl. Phys. 90 (2) 980 (2001).
[47] H. Iwata, U. Lindefelt, S. Oberg, and P. R. Briddon, Phys. Rev. B 65, 033203 (2001); Phys. Rev. B 68, 245309 (2003).
[48] T. G. Pedersen, K. Pedersen, and T. B. Kriestensen, Phys. Rev. B **63**, 20110 (2001).
[49] D. Vogel, P. Krüger, and J. Pollmann, Phys. Rev. B **52**, R14316 (1995); B **54**, 5495 (1996); B **55**, 12836 (1997).
[50] G. Litovchenko, Phys. Stat. Sol. B **162**, 447 (1990).
[51] G.L. Sun, I.G. Galben-Sandulache, T. Ouisse, J.M. Dedulle, M. Pons, R. Madar, D. Chaussende, Mat. Sci. For. 645-648 (2010) pp 63-66.
[52] Y. Ward, R. J. Young, R. A. Shatwell, J Mater Sci 42 (2007), p.5135-5141.
[53] D. Chaussende, F. Baillet, L. Charpentier, E. Pernot, M. Pons, R. Madar, J. Electrochem. Soc. Vol. 150, (2003), p. G653.
[54] D. Chaussende, F. Mercier, A. Boulle, F. Conchon, M. Soueidan, G. Ferro, A. Mantzari, A. Andreadou, E.K. Polychroniadis, C. Balloud, S. Juillaguet, J. Camassel, M. Pons, J. Cryst. Growth 310 (2008).
[55] S. Bai, R. P. Devaty, W. J. Choyke, U. Kaiser, G. Wagner, and M. F. MacMillan, Appl. Phys. Lett. 83, 3171 (2003).
[56] G. Zoulis, J. Sun, M. Beshkova, R. Vasiliauskas, S. Juillaguet, H. Peyre, M. Syvï£¡jï£¡rvi, R. Yakimova, J. Camassel, Mat. Sci. For. Vols. 645-648 (2010) pp 179-182.
[57] S. Ha, S. Skowronski, J.J. Sumakeris, M.J. Paisley, M.K. Kas Phys.Rev. Lett. Vol. 92, No. 17, 175504 (2004).

[58] B. J. Skromme, K. Palle, C. D. Poweleit, L. R. Bryant, W. M. Vetter, M. Dudley, K. Moore, and T. Gehoski, Mater. Sci. Forum 389-393, 455 (2002); B. J. Skromme, K. C. Palle, M. K. Mikhov, H. Meidia, S. Mahajan, X. R. Huang, W. M. Vetter, M. Dudley, K. Moore, S. Smith, and T. Gehoski, Mater. Res. Soc. Symp. Proc. 742, 181 (2003).
[59] J. Q. Liu, H. J. Chung, T. Kuhr, Q. Li, and M. Skowronski, Appl. Phys. Lett. 80, 2111 (2002).
[60] S. Izumi, H. Tsuchida, T. Tawara, I. Kamata, and K. Izumi, Mater. Sci. Forum 483-485, 323 (2005); S. Izumi, H. Tsuchida, I. Kamata, and T. Tawara, Appl. Phys. Lett. 86, 202108 (2005).
[61] H. Fujiwara, T. Kimoto, T. Tojo, and H. Matsunami, Appl. Phys. Lett. 87, 051912 (2005).
[62] A. Laref, S. Laref, Phys. Stat. Sol. B 245, N1, 89-100 (2008).
[63] I.G. Galben-Sandulache, G.L. Sun, J.M. Dedulle, T. Ouisse, R. Madar, M. Pons, D. Chaussende, Mat. Sci. For. 645-648 (2010) pp 55-58.
[64] L. Latu-Romain, D. Chaussende, C. Balloud, S. Juillaguet, L. Rapenne, E. Pernot, J. Camassel, M. Pons, R. Madar, Mat. Sci. Forum, vols. 527-529 (2006), pp. 99-102.
[65] A. A. Lebedev, P. L. Abramov, E. V. Bogdanova, S. P. Lebedev, D. K. Nelson, G. A. Oganesyan, A. S. Tregubova, R Yakimova, Semicond. Sci. Technol. 23, 075004 (2008).
[66] A. A. Lebedev, P. L. Abramov, N. V. Agrinskaya, V. I. Kozub, S. P. Lebedev, G. A. Oganesyan, A. S. Tregubova, D. V. Shamshur, and M. O. Skvortsova, J. Appl. Phys. 105, 023706 (2009).
[67] M. Skowronski and S. Ha, J. Appl. Phys. 99, 011101 (2006).
[68] Y. Ward, R. J. Young, R. A. Shatwell, J Mater Sci 42 (2007), p.5135-5141.
[69] T. Quisse, J. App. Phys. **75**, 2092 (1994).
[70] J. C. Slater and G.F. Koster, Phys. Rev **94**, 1498 (1954).
[71] P. Vogl and H. P. Hjalmarson, and J. D. Dow, J. Phys. Chem Solids **44**, 365 (1983).
[72] Y. C. Chang and D. E. Aspnes, Phys. Rev. B **41**, 12002 (1990).
[73] B. Wenzien, P. Käckell, F. Bechstedt, and G. Cappellini, Phys. Rev. B **52**, 10897 (1995).
[74] R. G. Humphreys, D. Bimberg, W. J. Choyke, Solid. State. Com . 39, 163 (1981).
[75] Landolt-Börnstein, *Numerical and Functional Relationships in Science and Technology*, edited by K. H. Hellwege (Spring-Verlag, Berlin, 1982).
[76] G.Theodorou, G. Tsegas, and E. Kaxiras, J. Appl. Phys **85**, 2179 (1999).
[77] N. Bernstein, H. J. Gotsis, D. A. Papaconstantopoulos, and M. J. Mehl, Phys. Rev. B**71**, 075203 (2005).
[78] G. Cubiotti, Yu. N. Kucherenko, and V. N. Antonov, J. Phys. Cond. Mat **9**, 165 (1997).
[79] J. Kuriplach, M. Sob, G. Brauer, W. Anwand, E.-M. Nicht, P. G. Coleman, and , N. Wagner, Phys. Rev. B **59**, 1948 (1999).
[80] P.J. Colwell and M.V. Klein, Phys. Rev. B 6, 498 (1972).
[81] N. T. Son et al., Appl. Phys. Lett **66**, 107 (1995).
[82] R. Kaplan, and R. J. Wagner, Solid State Com. **55**, 67 (1985).
[83] M. Willatzen, M. Cardona, and N. E. Christensen, Phys. Rev. B **51**, 13150 (1995).
[84] K, -H. Lee, C. H. Park, B. -H. Cheong, K. J. Chang, Solid State Commun. **92**, 869 (1994).

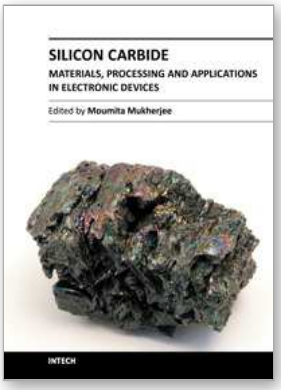

Silicon Carbide - Materials, Processing and Applications in Electronic Devices

Edited by Dr. Moumita Mukherjee

ISBN 978-953-307-968-4
Hard cover, 546 pages
Publisher InTech
Published online 10, October, 2011
Published in print edition October, 2011

Silicon Carbide (SiC) and its polytypes, used primarily for grinding and high temperature ceramics, have been a part of human civilization for a long time. The inherent ability of SiC devices to operate with higher efficiency and lower environmental footprint than silicon-based devices at high temperatures and under high voltages pushes SiC on the verge of becoming the material of choice for high power electronics and optoelectronics. What is more important, SiC is emerging to become a template for graphene fabrication, and a material for the next generation of sub-32nm semiconductor devices. It is thus increasingly clear that SiC electronic systems will dominate the new energy and transport technologies of the 21st century. In 21 chapters of the book, special emphasis has been placed on the â€œmaterialsâ€ aspects and developments thereof. To that end, about 70% of the book addresses the theory, crystal growth, defects, surface and interface properties, characterization, and processing issues pertaining to SiC. The remaining 30% of the book covers the electronic device aspects of this material. Overall, this book will be valuable as a reference for SiC researchers for a few years to come. This book prestigiously covers our current understanding of SiC as a semiconductor material in electronics. The primary target for the book includes students, researchers, material and chemical engineers, semiconductor manufacturers and professionals who are interested in silicon carbide and its continuing progression.

How to reference

In order to correctly reference this scholarly work, feel free to copy and paste the following:

Amel Laref and Slimane Laref (2011). Opto-Electronic Study of SiC Polytypes: Simulation with Semi-Empirical Tight-Binding Approach, Silicon Carbide - Materials, Processing and Applications in Electronic Devices, Dr. Moumita Mukherjee (Ed.), ISBN: 978-953-307-968-4, InTech, Available from: http://www.intechopen.com/books/silicon-carbide-materials-processing-and-applications-in-electronic-devices/opto-electronic-study-of-sic-polytypes-simulation-with-semi-empirical-tight-binding-approach

INTECH
open science | open minds

InTech Europe
University Campus STeP Ri
Slavka Krautzeka 83/A
51000 Rijeka, Croatia
Phone: +385 (51) 770 447

InTech China
Unit 405, Office Block, Hotel Equatorial Shanghai
No.65, Yan An Road (West), Shanghai, 200040, China
中国上海市延安西路65号上海国际贵都大饭店办公楼405单元
Phone: +86-21-62489820

Fax: +385 (51) 686 166
www.intechopen.com

Fax: +86-21-62489821